



CHORUS

This is the accepted manuscript made available via CHORUS. The article has been published as:

Lensinglike tensions in the Planck legacy release

Pavel Motloch and Wayne Hu

Phys. Rev. D **101**, 083515 — Published 10 April 2020

DOI: [10.1103/PhysRevD.101.083515](https://doi.org/10.1103/PhysRevD.101.083515)

Lensing-like tensions in the Planck legacy release

Pavel Motloch¹ and Wayne Hu²

¹*Canadian Institute for Theoretical Astrophysics, University of Toronto, M5S 3H8, ON, Canada*

²*Kavli Institute for Cosmological Physics, Department of Astronomy & Astrophysics,
Enrico Fermi Institute, University of Chicago, Chicago, Illinois 60637, U.S.A*

We analyze the final release of the Planck satellite data to constrain the gravitational lensing potential in a model-independent manner. The amount of lensing determined from the smoothing of the acoustic peaks in the temperature and polarization power spectra is 2σ too high when compared with the measurements using the lensing reconstruction and 2.8σ too high when compared with Λ CDM expectation based on the “unlensed” portion of the temperature and polarization power spectra. The largest change from the previous data release is the Λ CDM expectation, driven by improved constraints to the optical depth to reionization. The anomaly still is inconsistent with actual gravitational lensing, given that the lensing reconstruction constraints are discrepant independent of the model. Within the context of Λ CDM, improvements in its parameter constraints from lensing reconstruction brings this tension to 2.1σ and from further adding baryon acoustic oscillation and Pantheon supernova data to a marginally higher 2.2σ . Once these other measurements are included, marginalizing this lensing-like anomaly cannot substantially resolve tensions with low-redshift measurements of H_0 and S_8 in Λ CDM, Λ CDM+ N_{eff} or Λ CDM+ $\sum m_\nu$; furthermore the artificial strengthening of constraints on $\sum m_\nu$ is less than 20%.

I. INTRODUCTION

The standard cosmological model, Λ CDM, has been successful in describing a large number of diverse cosmological observations. Despite this phenomenological success, there are several hints Λ CDM might not be the end of the story. Most notable is the difference, statistically significant at over 5σ , between the values of the Hubble constant directly measured in the low-redshift Universe [1, 2] and indirectly extrapolated within the context of Λ CDM from the observations sensitive to the early Universe physics [3, 4] (see however [5, 6]). The tension between measurements of the amount of clustering in the late Universe from weak lensing observations [7–11] and from the Planck satellite [3] is of a more modest statistical significance, but has persisted over time. Given these differences between experimental constraints, it is crucial to search for possible systematic effects that could bias our inferences from individual observations.

Regarding the Planck satellite, there are several “curiosities”, such as difference in cosmological parameters when comparing constraints from different ranges of angular scales [12, 13] and the large scale anomalies (see [14] for an overview), that could potentially shed some light on the detected discrepancies.

This work is motivated by another such “curiosity” in the Planck data, the so-called oscillatory residuals between the Planck temperature power spectra and the best-fit Λ CDM model, visible between angular multipoles ℓ of roughly 900 and 1700 [13, 15]. In this range of angular scales, these residuals are roughly of opposite phase to the CMB peaks and are thus somewhat degenerate with the effects of gravitational lensing. The amount of gravitational lensing inferred from the temperature and polarization power spectra is then anomalously high and this affects constraints on cosmological parameters. In this context, the oscillatory residual curiosity is usually

referred to as the A_L or lensing anomaly in the power spectra. Various aspects of this anomaly have been extensively studied [12, 13, 16–28].

In [29], we used the 2015 release of the Planck data [30] to investigate this anomalously high lensing power in depth within the framework of model-independent lensing constraints. We allowed gravitational lensing potentials beyond the Λ CDM model and studied implications of such deviations. Recently, the legacy version of the Planck collaboration products was released, with large and small scale polarization data finally deemed to be sufficiently systematics free to be useable for a cosmological analysis. It is thus timely to reevaluate our previous analysis with the new data and make definitive model-independent statements about the gravitational lensing constraints from Planck, including a final assessment of the significance of various tensions found in the data. We also show how fully marginalizing parameters associated with the lensing anomaly in the power spectra affects selected cosmological parameters of interest in Λ CDM and two of its extensions, Λ CDM + N_{eff} and Λ CDM + $\sum m_\nu$.

This paper is organized as follows: We start by summarizing the data and likelihoods used in this work in § II. In § III we briefly review the technique for probing the gravitational lensing potential in a model-independent fashion and in § IV provide details of our Markov Chain Monte Carlo (MCMC) analysis. § V presents lensing constraints derived from the Planck likelihoods and § VI assesses the effects the Planck lensing anomaly has on constraints of cosmological parameters. We conclude with discussion in § VII. In the Appendix, we justify our choice of tension statistic with a multidimensional analysis.

II. DATA AND LIKELIHOODS

To constrain values of cosmological parameters, we mainly use likelihoods derived from data collected by the Planck satellite. All Planck likelihoods used in this work are listed in Table I.

We primarily use the legacy versions of the temperature, polarization and lensing likelihoods [31, 32]. To better constrain cosmological parameters, especially τ , small scale temperature and polarization likelihoods are always accompanied by the large scale TT and EE likelihoods. We also investigate how some of our results change when we replace the official Planck large scale EE likelihood by its post-legacy version based on a reanalysis of the Planck High Frequency Instrument (HFI) data [33].

We compare the new constraints with their counterparts based on the likelihoods included in the second Planck data release [30, 34]. This older release included information from the large scale TE and BB power spectra which we do not use in the legacy analysis, but this does not significantly affect constraints on the gravitational lensing potential.

For certain analyses we additionally use baryon acoustic oscillation likelihoods (BAO) from [35–37], Pantheon supernova likelihood (SN) [38] and the South Pole Telescope (SPT) TE and EE power spectra likelihood [39].

III. LENSING PARAMETERIZATION

In this work we apply a technique to directly constrain the CMB gravitational lensing potential from the CMB data in a model-independent way. In this section we provide a brief overview of this technique, while more details can be found in [40, 41].

We parameterize the gravitational lensing potential power spectrum in terms of N_{pc} effective parameters $\Theta^{(i)}$,

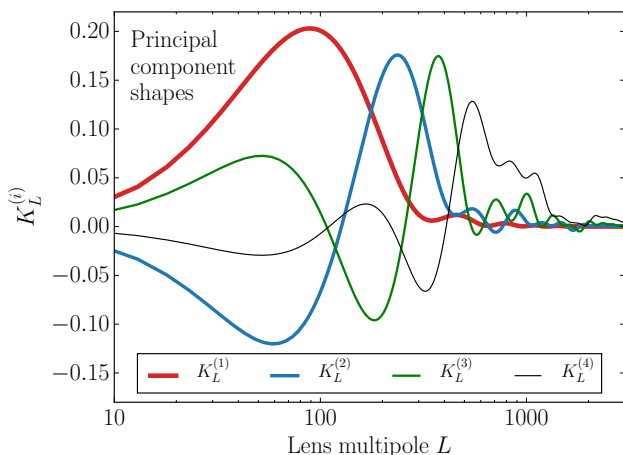


FIG. 1. Lensing principal components $K_L^{(i)}$ used in this work.

which determine arbitrary variations around a fixed fiducial power spectrum $C_{L,\text{fid}}^{\phi\phi}$ as

$$C_L^{\phi\phi} = C_{L,\text{fid}}^{\phi\phi} \exp \left(\sum_{i=1}^{N_{\text{pc}}} K_L^{(i)} \Theta^{(i)} \right). \quad (1)$$

In this setup, constraining $\Theta^{(i)}$ from the data corresponds directly to constraining the gravitational lensing potential. This should be contrasted with the common approach of introducing a phenomenological parameter A_L which multiplies $C_L^{\phi\phi}$ at each point in the model space and cannot be interpreted in terms of the lensing potential once model parameters are marginalized over.

To allow easier comparison with our previous results, we use the same $C_{L,\text{fid}}^{\phi\phi}$ and $K_L^{(i)}$ as in [29]. The fiducial cosmological model used to calculate $C_{L,\text{fid}}^{\phi\phi}$ in Eq. (1) is taken from the best fit flat Λ CDM cosmological model, determined from the Planck 2015 TT+lowl likelihoods, with no primordial tensor modes and minimal mass neutrinos ($\sum m_\nu = 60$ meV).

Table II lists values of the corresponding cosmological parameters; the symbols have their standard meaning: $\Omega_b h^2$ is the physical baryon density; $\Omega_c h^2$ the physical cold dark matter density; n_s the tilt of the scalar power spectrum; $\ln A_s$ its log amplitude at $k = 0.05$ Mpc $^{-1}$; τ the optical depth through reionization, and θ_* the angular scale of the sound horizon at recombination. To reflect the best constraints on τ at the time, its value was taken from [42] and A_s decreased to keep $A_s e^{-2\tau}$ constant.

While a lower A_s tends to exacerbate the preference for anomalously high lensing in the temperature power spectrum within the Λ CDM context, here it serves only to define the baseline fiducial model against which $\Theta^{(i)}$ are measured and does not affect the significance of tensions discussed below. If we used a different fiducial model to define $C_{L,\text{fid}}^{\phi\phi}$, for example one based on the Planck 2018 data, each $\Theta^{(i)}$ parameter would be shifted by a constant, the value of which would depend on the ratio of the two fiducial $C_L^{\phi\phi}$. For example, in Fig. 2 this would lead to a coherent shift of the contours relative to the origin, but the tensions between datasets would remain unchanged due to the coherent nature of this shift.

The $K_L^{(i)}$ in (1) are chosen such that $\Theta^{(i)}$ correspond to the N_{pc} principal components (PCs) of the gravitational lensing potential best measured by Planck 2015 temperature data, as determined using a Fisher matrix construction [29]. The resultant eigenmodes $K_L^{(i)}$ are shown in Fig. 1. We retain $N_{\text{pc}} = 4$ PCs in order to fully characterize all sources of lensing information [29].

TABLE I. Planck likelihoods used in this work

Label	Release	Power spectra	ℓ -range	Name
TT	legacy	TT	$\ell \geq 30$	plik_rd12_HM_v22_TT
	2015	TT	$\ell \geq 30$	plik_dx11dr2_HM_v18_TT
TTTEEE	legacy	TT,TE,EE	$\ell \geq 30$	plik_rd12_HM_v22b_TTTEEE
	2015	TT,TE,EE	$\ell \geq 30$	plik_dx11dr2_HM_v18_TTTEEE
lowl	legacy	TT,EE	$\ell < 30$	commander_dx12_v3_2_29, simall_100x143_offlike5_EE_Aplanck_B
	2015	TT,TE,EE,BB	$\ell < 30$	lowl_SMW_70_dx11d_2014_10_03_v5c_Ap
sroll12	post-legacy	TT,EE	$\ell < 30$	commander_dx12_v3_2_29, simall_100x143_sroll12_v3_EE_Aplanck
PP	legacy	$\phi\phi$	$8 \leq \ell \leq 400$	smicadx12_Dec5_ftl_mv2_ndclpp_p_teb_consext8_CMBmerged
	2015	$\phi\phi$	$40 \leq \ell \leq 400$	smica_g30_ftl_full_pp

TABLE II. Λ CDM parameters and their fiducial values for the lens PC construction^a.

Parameter	Fiducial value
$100 \theta_*$	1.041
$\Omega_c h^2$	0.1197
$\Omega_b h^2$	0.02223
n_s	0.9658
$\ln(10^{10} A_s)$	3.049
τ	0.058

^a In Λ CDM, these parameters also imply a Hubble constant of $h = 0.6733$.

IV. MCMC ANALYSIS

We use CosmoMC^{*1} [43] to sample the posterior probabilities in the various parameter spaces. Each of our chains has a sufficient number of samples such that the Gelman-Rubin statistic $R - 1$ [44] falls below at least 0.01.

We assume flat tophat priors on $\Theta^{(i)}$ and choose an uninformative prior on $\Theta^{(1)}$, as it is the variable in which we will evaluate the tensions between data sets. As the lensing reconstruction constraint on $\Theta^{(2)}$ is still somewhat informative, we restrict $\Theta^{(2)}$ to lie within six standard deviations from its mean value, both obtained from the Planck lensing reconstruction likelihood. For consistency with our previous work, this prior is based on the 2015 release of the likelihood. This prior does not significantly change any of the tensions we find below. For the remaining two $\Theta^{(i)}$, that allow further freedom in the shape of the gravitational lensing potential, we limit their variation such that all $C_L^{\phi\phi}$ are within a factor of 1.5 of $C_{L,\text{fid}}^{\phi\phi}$. These weak priors are meant to eliminate cases that would be in conflict with other measurements

TABLE III. Flat $\Theta^{(i)}$ priors used in this work.

Parameter	Prior range
$\Theta^{(1)}$	[-2.00, 2.00]
$\Theta^{(2)}$	[-2.10, 1.67]
$\Theta^{(3)}$	[-2.32, 2.32]
$\Theta^{(4)}$	[-3.16, 3.16]

of large scale structure or imply unphysically large amplitude high frequency features in $C_L^{\phi\phi}$. Table III summarizes the ranges over which we allow $\Theta^{(i)}$ to vary.

In analyses that include CMB temperature and polarization power spectra, in addition to the four lensing parameters $\Theta^{(i)}$ we also vary the six Λ CDM parameters (or more in the extensions), with flat uninformative priors. Unlike the standard analysis, these parameters do not affect the lensing potential $C_L^{\phi\phi}$ used to calculate the lensed CMB temperature and polarization power spectra and only affect the unlensed power spectra at recombination. Sometimes, we will refer to these parameters collectively as $\tilde{\theta}_A$, where the tilde is to remind the reader that the gravitational lens potential entering the calculation of the lensed CMB power spectra is not changed by these parameters but is fully determined by $\Theta^{(i)}$ through (1).

Given constraints on the parameters $\tilde{\theta}_A$ and assuming a particular cosmological model, for instance Λ CDM, it is possible to make a prediction of the values of $\Theta^{(i)}$, which then can be compared with the direct constraints.

In our analysis, the lensing parameters $\Theta^{(i)}$ serve two distinct purposes. In § V we use them to constrain $C_L^{\phi\phi}$ and study tensions between various sources of lensing information in the data, while in § VI we use $\Theta^{(i)}$ as nuisance parameters to marginalize over and remove the lensing-like anomaly in the temperature and polarization power spectra to uncover its effects on cosmological parameters. In particular, in the former case PP is used to directly constrain $\Theta^{(i)}$ through (1). In the latter PP

^{*1} <https://github.com/cmbant/CosmoMC>

depends on the parameters $\tilde{\theta}_A$ of the investigated model in the usual manner, which allows us to constrain these parameters better. This then indirectly improves lensing parameter constraints from the temperature and polarization power spectra as we shall see.

We use default foreground and nuisance parameters and their priors in all the likelihoods.

V. LENSING CONSTRAINTS FROM THE FINAL PLANCK RELEASE

In Fig. 2 we show constraints on $\Theta^{(1)}, \Theta^{(2)}$ that parameterize the CMB gravitational lensing potential in a model independent manner. We compare here the direct constraints on $\Theta^{(1,2)}$ from the TTTEEE+low ℓ (red) and PP (blue) likelihoods with the Λ CDM predictions (green) based on the TTTEEE+low ℓ constraints on $\tilde{\theta}_A$, the standard cosmological parameters constrained only through their effect on the unlensed power spectra. In Fig. 3 we show the same, with the information from the small scale polarization dropped, i.e. TTTEEE replaced by TT.

The amount of lensing manifested in the high- ℓ temperature and polarization likelihoods is notably higher than the amount of lensing inferred from the lensing reconstruction or the one predicted within Λ CDM as evidenced from the barely overlapping 95% confidence level (CL) regions. As expected, the TT+low ℓ / TTTEEE+low ℓ data can directly constrain only the leading lensing principal component $\Theta^{(1)}$ and do not provide competitive constraints on $\Theta^{(2)}$ (or the higher lensing PCs). By construction, the two lensing PCs are also mostly uncorrelated for these two cases (red contours). As discussed in [45], the degeneracy direction in the Λ CDM predictions (green contours) is closely related to changes in the lensing potential produced by shifts in A_s and $\Omega_c h^2$, the two parameters on which $C_L^{\phi\phi}$ mainly depends in Λ CDM.

In Figs. 2 and 3 we use dashed contours to denote the same probability contours derived using the 2015 Planck data. The direct constraints from the smoothing of the acoustic peaks (red) do not significantly change, which is not surprising given only minor changes in the high- ℓ Planck likelihoods and insensitivity of $\Theta^{(1,2)}$ constraints to the details of the low- ℓ likelihoods [29]. The lensing reconstruction constraints (blue) are weakened, because in the legacy release the Planck “lensing only” likelihood adds marginalization over the uncertainties in the cosmological parameters, that affect lensing bias subtractions. The largest changes are in the predictions within the context of the Λ CDM model (green); these mostly reflect changes in τ constraints and the related breaking of the $A_s e^{-2\tau}$ degeneracy of the high- ℓ data.

In Fig. 4 we show the constraints on $\Theta^{(1)}$, marginalized over all the other parameters. Using these posterior probability distributions, we calculate the significance of tensions between the various constraints. Because the posteriors are non-Gaussian, we use the generalization of

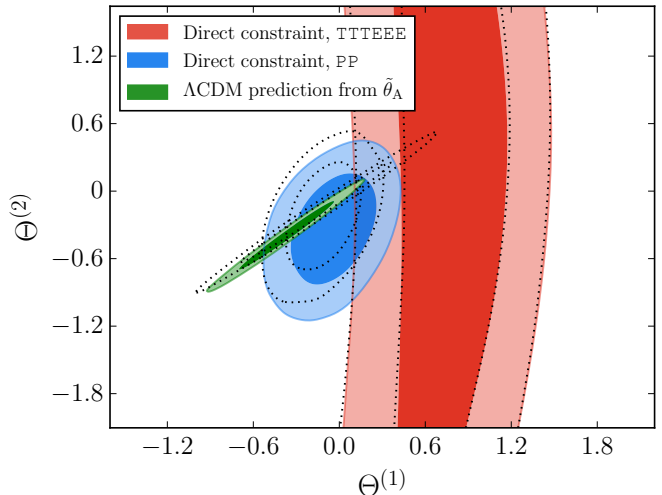


FIG. 2. CMB power spectrum constraints on lens PCs $\Theta^{(1)}$ and $\Theta^{(2)}$ from TTTEEE+low ℓ (red, 68% and 95% CL) compared with lens reconstruction PP (blue) and Λ CDM predictions based on unlensed parameters $\tilde{\theta}_A$ from TTTEEE+low ℓ (green). Dashed contours show the constraints when using the 2015 likelihoods.

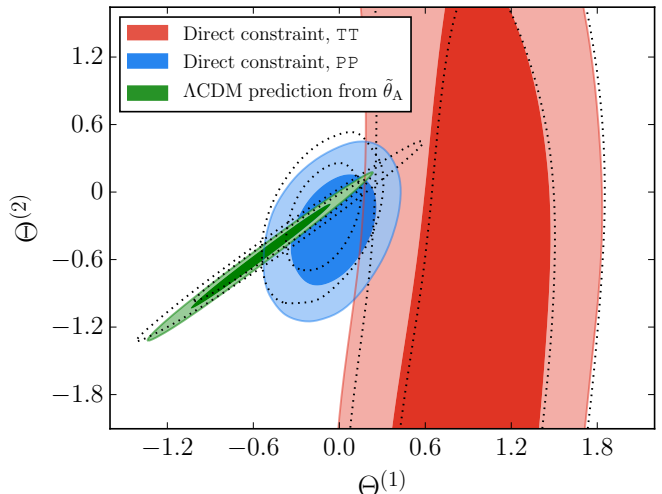


FIG. 3. Same as Fig. 2, but with high- ℓ polarization data neglected, i.e. TTTEEE+low ℓ is replaced by TT+low ℓ .

the “shift in the means” statistic to non-Gaussian posteriors, introduced in Appendix C of [45]. Note that the choice to investigate tensions in $\Theta^{(1)}$, the only such parameter to be significantly constrained by the temperature and polarization power spectra – as opposed to some function of $\Theta^{(i)}$ with free parameters – was made a priori and so we do not have to consider the look-elsewhere effect, despite adding four new parameters.

Comparing the direct constraints from TTTEEE+low ℓ (red in Fig. 4) with either the lensing reconstruction constraints from PP (blue) or the Λ CDM prediction based on

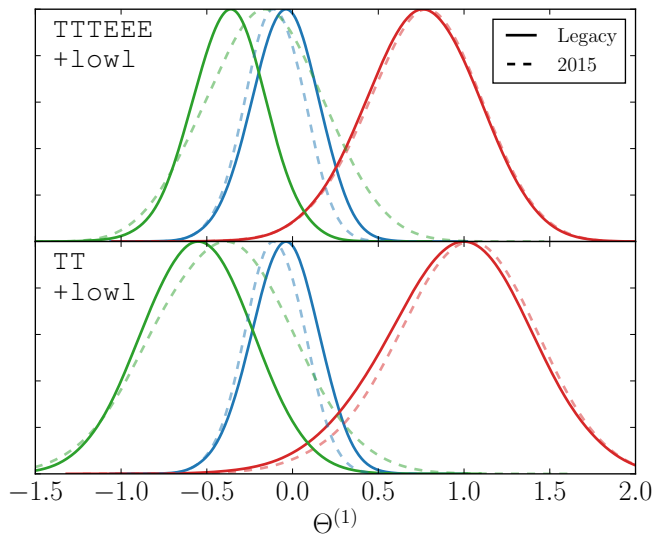


FIG. 4. Posterior probability distributions for $\Theta^{(1)}$. Direct constraints from PP (blue), direct constraints from **TTTEEE+lowl** (red, top) or **TT+lowl** (red, bottom) and Λ CDM predictions based on constraints on the “unlensed” cosmological parameters θ_A from **TTTEEE+lowl** (green, top) or **TT+lowl** (green, bottom). Solid curves correspond to constraints obtained with the Planck legacy likelihoods, dashed with the 2015 version of the likelihoods.

the constraints on the “unlensed” cosmological parameters θ_A (green), we find tensions of 2.0σ and 2.8σ respectively. While the latter is closely related to the usually discussed A_L tension, the former shows that the amount of peak smoothing in Planck power spectra is somewhat unusual also when compared with the lensing reconstruction. Dropping the high- ℓ polarization data changes the respective tensions to 2.1σ and 2.7σ .

In Appendix A, we confirm the $\sim 2\sigma$ tension between the direct constraints from **TTTEEE+lowl** and PP using update difference in mean statistic developed in [20]. This statistic was developed to investigate tensions that involve a data set that is constraining only a subset of the parameters (**TTTEEE+lowl** strongly constraining only $\Theta^{(1)}$ in our case). This result shows that marginalizing over other $\Theta^{(i)}$ does not artificially degrade significance of the discovered tension.

Given that the **TTTEEE+lowl** and PP constraints are in tension even when allowing arbitrary $C_L^{\phi\phi}$, while the Λ CDM prediction is in good agreement with the latter, it is not likely that gravitational lensing is responsible for the lensing-like anomaly.

In Fig. 5, we show the effect of replacing the official Planck low- ℓ EE likelihood with **sroll12**, an improved analysis of the Planck HFI polarization data [33]. The tension between the direct constraints on $\Theta^{(1)}$ from the smoothing of the peaks and the Λ CDM expectation in this case decreases to 2.5σ , both when high- ℓ polarization is present or absent. This is due to an increased best fit value of τ (see [33] for a similar discussion within the

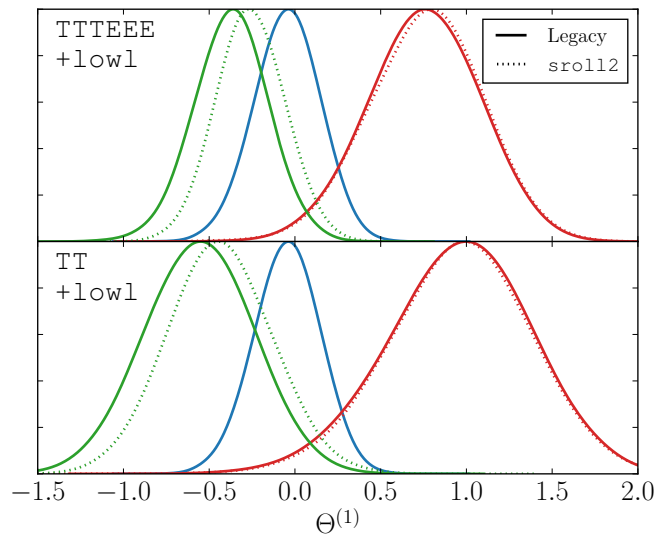


FIG. 5. Effect of the reanalysis of the large scale Planck HFI data. The solid curves as in Fig. 4, the dotted curves show effects of replacing the official Planck large scale EE likelihood with the **sroll12** likelihood from [33].

context of the A_L parameter).

Because the direct constraints on the lensing principal components $\Theta^{(i)}$ from the Planck temperature and polarization power spectra do not notably change, the significances of the tensions with the SPT data presented in [45] change by less than 0.1σ . The tension between lensing constraints from Planck high- ℓ temperature power spectra and lensing constraints from SPT TE and EE power spectra remains at 3.0σ , adding Planck polarization decreases the significance to 2.9σ .

Related to this, let us comment on a possibility of the Planck lensing-like anomaly being driven by new physics at recombination that changes the CMB temperature and polarization power spectra in a way similar to lensing. If this was the case, we would expect SPT temperature and polarization data to also show preference for high amount of lensing. However, this data actually prefers somewhat lower amplitude than the Planck lensing reconstruction, although with large error bars [45].

VI. COSMOLOGICAL PARAMETER IMPACT

If, despite significant care and effort of the Planck Collaboration, the observed lensing-like anomaly fully or partially originates in an unknown systematic effect, constraints on cosmological parameters would be directly affected. In this section, we comment on how the preference for anomalously high lensing amplitude in the Planck temperature and polarization power spectra affects constraints on selected cosmological parameters, especially in the context of parameter tensions with other experiments.

In this section, $\Theta^{(i)}$ only enter the $C_L^{\phi\phi}$ used to calculate the temperature and polarization power spectra; the PP likelihood uses the standard $C_L^{\phi\phi}$ of the given cosmological model, evaluated using $\hat{\theta}_A$. This way, marginalizing over $\Theta^{(i)}$ removes any effect of the extra peak smoothing and other lensing effects in the temperature and polarization power spectra on constraints of the cosmological parameters. This generalizes marginalization over A_L that is usually employed for this purpose.

We study Λ CDM and two of its extensions, where either N_{eff} , the effective number of light relativistic degrees of freedom, or $\sum m_\nu$, the sum of the neutrino masses, are allowed to vary.

A. Λ CDM

Within the context of Λ CDM, the anomalously high lensing power in temperature and polarization power spectra acts towards increasing the best fit values of $\Omega_c h^2$ and A_s . Due to parameter degeneracies, this leads to related shifts in $\Omega_b h^2$, H_0 and n_s . Once the lensing PCs are allowed to absorb the extra lensing, all the cosmological parameter readjust accordingly. Notably, $\Omega_c h^2$ shifts from the Λ CDM value 0.1202 ± 0.0014 to $\Omega_c h^2 = 0.1179 \pm 0.016$. This then affects the interpretation of tensions with local measurements.

In the top of Fig. 6, we show changes to constraints on the current value of the Hubble constant H_0 and the parameter $S_8 = \sigma_8 \sqrt{\Omega_m}/0.3$, that are the parameters involved in the most significant tensions with other cosmological experiments. Here $\Omega_m = \Omega_c + \Omega_b$ and σ_8 is the linear-theory root mean square fluctuations in spheres with a radius of $8 h^{-1}$ Mpc at redshift $z = 0$. For reference, recent low-redshift measurements are $H_0 = (74.03 \pm 1.42)$ km/s/Mpc [1] and $S_8 = 0.783_{-0.025}^{+0.021}$ [7].

For both parameters, the anomalously high lensing power in the Planck temperature and polarization power spectra acts in the direction of increasing the tension, although for H_0 , this contribution is far from enough to explain majority of the observed discrepancy. When using TTTEEE+lowl, the parameters shift less, in part due to preference of the polarization data for lower values of H_0 unrelated to gravitational lensing [15].

As the H_0 tension can be restated in terms of disagreement in measurements of the comoving size of the sound horizon to the drag epoch r_d [46, 47], in Fig. 6 we also show constraints on this parameter. Notice that even though H_0 increases when lensing is marginalized, r_d and the sound horizon get larger. This is in the opposite direction than what is required for relieving H_0 tension in the inverse distance ladder. This is because the acoustic peak positions still fix $\Omega_m h^3$ so that raising H_0 lowers $\Omega_m h^2$ (see Fig. 7).

Correspondingly, in the same Figure we see that when we add BAO, supernova constraints, and Planck lensing reconstruction, which are the observables that are consistent with the Planck best fit cosmology, the parameters

shift back towards their Λ CDM values. The net shifts from marginalizing over the lensing anomaly end up being much smaller than the observed tensions.

Overall, in the context of Λ CDM it is thus possible to conclude that better understanding of the Planck lensing-like anomaly will not play an important role in resolution of the observed tensions.

Assuming Λ CDM is the correct cosmological model, we can also revisit the significance of the $\Theta^{(1)}$ tension discussed in the previous section. While previously we used only the “unlensed” part of TTTEEE+lowl to constrain the values of θ_A , we can now fold in the PP information, to better constrain these θ_A parameters. This allows us to make tighter predictions on $\Theta^{(i)}$ within the context of Λ CDM. Compared with this improved Λ CDM prediction, the direct measurement of $\Theta^{(1)}$ from the smoothing of the acoustic peaks is only 2.1σ anomalous. This is a fairer quantification of the Planck lensing-like tension in Λ CDM than just looking at the internal tension in the temperature and polarization power spectra (or A_L in the usual approach), because now we are taking all of the Planck data into consideration. Alleviation of the tension comes mostly from shifting $\Omega_c h^2$ back up to 0.1192 ± 0.0012 , which in Λ CDM increases the predicted lensing power. Additionally, raising $\Omega_c h^2$ lowers radiation driving, which smooths the acoustic peaks. This reduces the oscillatory residuals, lowering the direct constraint on $\Theta^{(1)}$.

After adding BAO and SN data to improve the Λ CDM prediction further, the tension goes mildly up, to 2.2σ . We do not use local measurements of H_0 or weak lensing measurements in making the prediction because of the aforementioned tensions.

B. Λ CDM + N_{eff}

Adding light relativistic degrees of freedom to the early Universe has been investigated as a possible avenue to reduce the H_0 tension. Additionally, constraints on N_{eff} are one of the main science drivers for the proposed CMB-S4 experiment [48]. This motivates us to investigate how much does the Planck lensing-like anomaly affect parameter constraints in this model.

In Fig. 7, we focus on TT+lowl data and show constraints on $\Omega_m h^3$ and H_0 in Λ CDM and Λ CDM + N_{eff} , with and without marginalization over the lensing PCs $\Theta^{(i)}$. It is visible that allowing arbitrary gravitational lensing shifts the contour along the CMB $\Omega_m h^3$ degeneracy, while releasing N_{eff} from its fiducial value opens up this degeneracy direction. When using only the TT+lowl data, this combination of lensing marginalization and degeneracy breaking allows an increase of H_0 to (71.5 ± 3.2) km/s/Mpc. However, as in Λ CDM, since lensing mainly allows shifts at fixed $\Omega_m h^3$, adding BAO, Pantheon supernovae and CMB lensing reconstruction brings H_0 down to (68.3 ± 1.4) km/s/Mpc, because the corresponding constraints on Ω_m are consistent with the Planck best fit val-

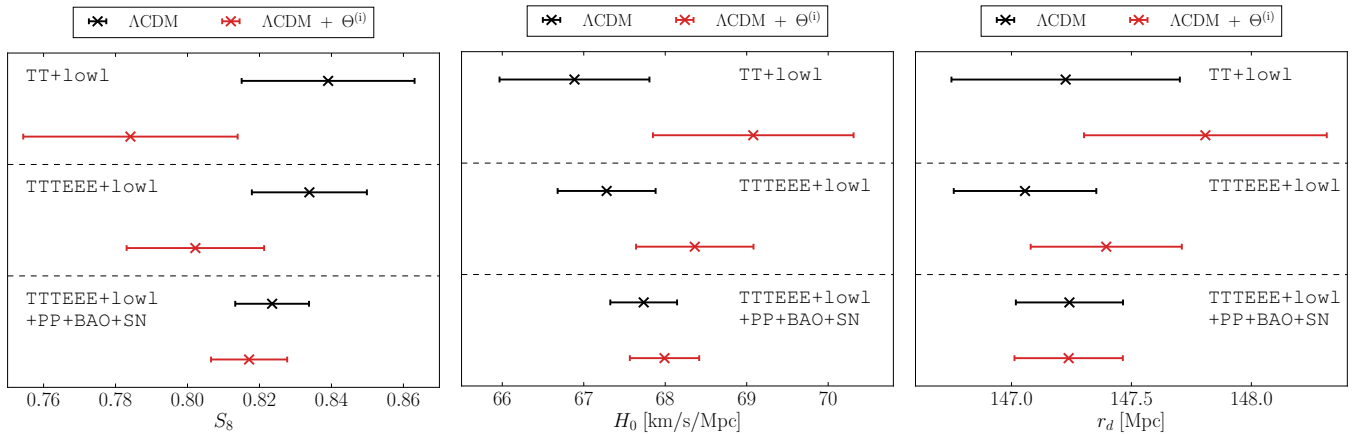


FIG. 6. Impact of marginalizing over the lensing anomaly on Λ CDM tension parameters. Constraints on S_8 (left), H_0 (center) and r_d (right) from TT+lowl (top), TTTEEE+lowl (middle) or TTTEEE+lowl+PP+BAO+SN (bottom) with (red) and without (black) marginalizing over the lensing information contained in the smoothing of the peaks of the temperature and polarization power spectra.

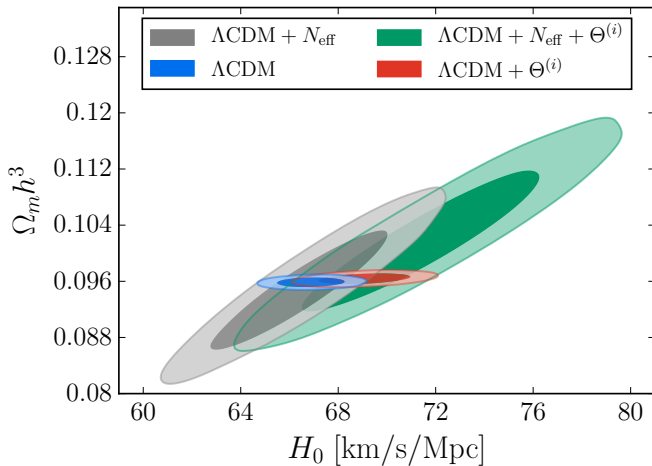


FIG. 7. TT+lowl constraints on $\Omega_m h^3$ and H_0 in Λ CDM with (red) and without (blue) marginalizing over the lensing anomaly. In green and gray respectively, we show the same constraints in Λ CDM+ N_{eff} .

ues. For TTTEEE+lowl the situation is qualitatively similar, but already with TTTEEE+lowl alone the marginalization over $\Theta^{(i)}$ pushes H_0 to only (68.2 ± 1.6) km/s/Mpc.

As for N_{eff} itself, we find its best fit value to be within one standard deviation away from the standard model value 3.046 for all the cases we study both with and without the lensing PCs $\Theta^{(i)}$ marginalized, see Fig. 8.

C. Λ CDM + $\sum m_\nu$

When using only the CMB temperature and polarization power spectra, the most constraining effect of neutrino masses is suppression of $C_L^{\phi\phi}$ below the neutrino

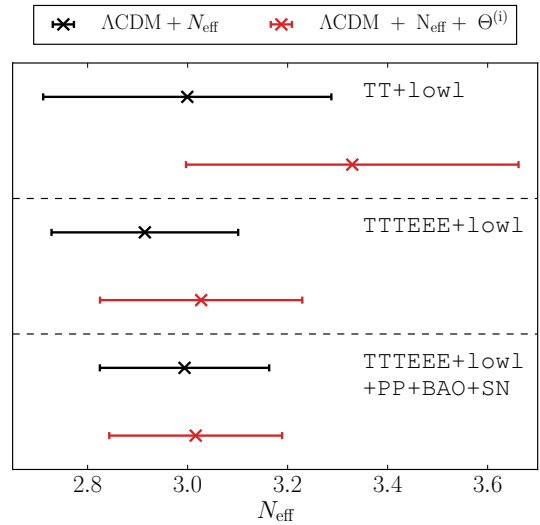


FIG. 8. Impact of marginalizing over Planck lensing anomaly on N_{eff} . Constraints from TT+lowl (top), TTTEEE+lowl (middle) or TTTEEE+lowl+PP+BAO+SN (bottom) with (red) and without (black) marginalizing over the lensing anomaly.

free-streaming scale, which lowers the amount of smoothing of the acoustic peaks. With our methodology, this is easy to see. After marginalizing over $\Theta^{(i)}$, the constraints on $\sum m_\nu$ degrade significantly, with the upper 95% CL increasing from 0.57 eV to 1.1 eV when using TT+lowl and from 0.26 eV to 0.87 eV when using TTTEEE+lowl (see Fig. 9 for the latter).

Conversely in Λ CDM + $\sum m_\nu$, the lensing-like anomaly strengthens the constraints on neutrino masses, as positive neutrino masses exacerbate the tension. To estimate importance of the anomaly in this context, in Fig. 9 we show constraints on $\sum m_\nu$ using TTTEEE+lowl+PP+BAO+SN, i.e. when additionally includ-

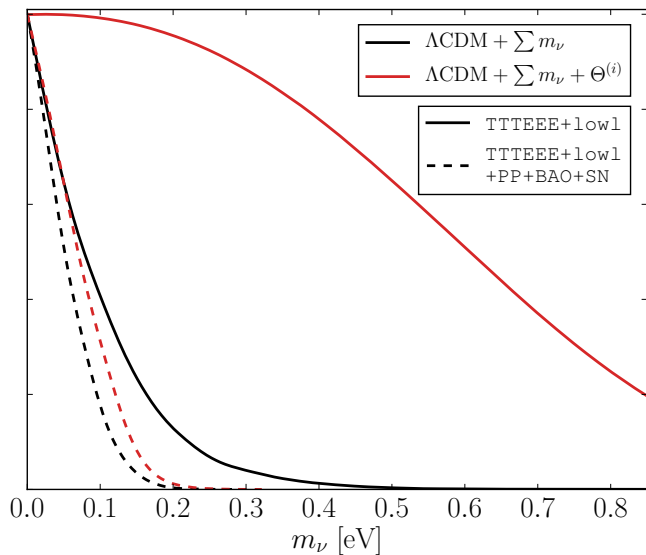


FIG. 9. Constraints on $\sum m_\nu$ using TTTEEE+lowl (solid) and TTTEEE+lowl+PP+BAO+SN (dashed) with (red) and without (black) marginalizing over the lensing anomaly.

ing Planck lensing reconstruction, together with BAO and SN data. We find that not using the information contained in the amount of peak smoothing (by marginalizing over $\Theta^{(i)}$) degrades the neutrino constraint by about 20%, from the 95% upper CL of 0.115 eV to 0.134 eV.

The sum of the neutrino masses is well constrained even without the knowledge of the amount of peak smoothing in the temperature and polarization power spectra. This is due to different parameter degeneracy directions: the BAO+SN data is sensitive to the sum of CDM and neutrino energy densities, while to increase the lensing power in PP it is necessary to either increase $\Omega_c h^2$ or decrease the sum of the neutrino masses.

We also checked that in the full TTTEEE+lowl+PP+BAO+SN data set, considering non-flat cosmologies further degrades the constraint on $\sum m_\nu$ by only about 10%, again because of a degeneracy breaking (see Fig. 10). While the lensing anomaly can be translated into a preference for a closed Universe when considering the temperature and power spectra alone, as recently emphasized by [19], we find that adding either Planck lensing reconstruction or BAO+SN leads to results consistent with flat Universe. This preference is robust with respect to whether one marginalizes over the lensing anomaly or not.

VII. DISCUSSION

In this work we studied constraints on CMB gravitational lensing potential from the final release of the Planck satellite data. The results are consistent with our previous analysis of an earlier release of the data. The biggest change in the final release are improved con-

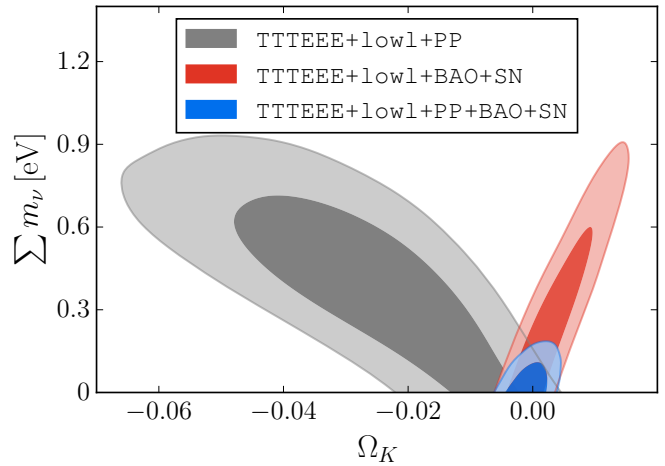


FIG. 10. Constraints on the sum of the neutrino masses and the curvature density parameter Ω_K after marginalizing the lensing anomaly in Λ CDM+ Ω_K + $\sum m_\nu + \Theta^{(i)}$ for various combinations of data sets.

straints on the optical depth to recombination τ , that then improve the prediction of the lensing power expected within the Λ CDM model.

The overall picture remains the same: allowing for an arbitrary gravitational lensing potential still leads to anomalously high lensing power determined from the smoothing of the peaks in the temperature and polarization power spectra. This power is about 2σ higher than the lensing power measured directly through the reconstruction of the gravitational lensing potential and close to 3σ higher when compared with the Λ CDM prediction based on values of the standard cosmological parameters constrained only through their effect on the unlensed power spectra (see Fig. 4). The latter is related to the usually quoted A_L tension and is associated with the oscillatory residuals in the temperature power spectrum.

Because these oscillatory residuals in conjunction with the low multipole anomalies also impact Λ CDM parameters in a manner that exacerbates tension [13, 15], we can make a better Λ CDM prediction by combining parameter constraints from Planck lensing reconstruction, BAO, SN and the “unlensed” portion of TTTEEE+lowl (marginalizing over the lensing information $\Theta^{(i)}$ in the CMB power spectra). Compared with this joint prediction, the amount of the gravitational lensing inferred from smoothing of the CMB acoustic peaks in Planck data is only anomalous in Λ CDM at 2.2σ , comparable to the model independent value.

It should also be noted that when analyzing the Planck data using the CamSpec likelihood that is not currently publicly available, the significance of the A_L anomaly drops by approximately 0.5σ [3, 49]. Repeating our analysis with the CamSpec likelihood could thus find a consistency at better than 2σ .

It is possible that such levels of discrepancy can be caused by a random fluctuation. Even taken at face

value, gravitational lensing is an unlikely cause of the A_L tension given that the two CMB sources of lensing information are discrepant for any lens power spectrum and that lensing reconstruction results are fully consistent with the Λ CDM expectation. Furthermore, as both SPT temperature and E -polarization data show preference for low amounts of lensing, it does not seem likely that physics beyond the standard model that only affects the temperature and/or polarization power spectra is the culprit, unless fine tuned to predominantly affect the range of scales where Planck is the most sensitive to lensing effects.

Consequently, we also studied what impact marginalizing this lensing-like anomaly has on constraints of cosmological parameters. When using only the temperature and large scale polarization Planck data, this reduces the tensions with the local measurements of H_0 and S_8 . However, additional data strongly restricts the ability of this lensing-like anomaly to shift cosmological parameters within Λ CDM. In this context, better understanding of Planck lensing-like anomaly is thus not likely to shed more light on the H_0 and S_8 tensions.

We also investigated Λ CDM+ N_{eff} and Λ CDM+ $\sum m_\nu$, with similar conclusions. In Λ CDM+ N_{eff} , the extra freedom in N_{eff} changes the relationship between $\Omega_m h^3$ and H_0 required by CMB power spectra data, however marginalizing lensing mainly broadens the H_0 constraints at fixed $\Omega_m h^3$ and hence constraints on Ω_m from data sets such as BAO, PP and SN drive the values of H_0 back to those found without marginalizing.

As is well known, the Planck lensing-like anomaly strengthens neutrino mass constraints. When combining Planck data with current BAO and SN data, we find that the lensing-like anomaly improves the neutrino mass constraints by less than 20%. Additionally allowing nonzero curvature further degrades this constraint by only about 10%. We find that when considering either PP or BAO+SN on top of Planck temperature and polarization power spectra, the data is consistent with flat Universe and this preference is not affected by the lensing anomaly.

In the future, additional data from experiments such as Simons Observatory and South Pole Telescope will improve our knowledge of the CMB, allowing us to better determine whether this lensing-like anomaly is indeed

just a statistical fluctuation or requires a more fundamental explanation.

ACKNOWLEDGMENTS

We thank Tom Crawford, Cora Dvorkin, Silvia Galli, Marco Raveri, and Kimmy Wu for useful discussions. WH was supported by U.S. Dept. of Energy contract DE-FG02-13ER41958 and the Simons Foundation. This work was completed in part with resources provided by the University of Chicago Research Computing Center.

Appendix A: Tension in Multiple Dimensions

In the main paper, we quantify the tension between the PP and TTTEEE+lowl datasets in a single parameter $\Theta^{(1)}$ with 3 other $\Theta^{(i)}$ parameters marginalized. In this Appendix we address the question of whether this single parameter accurately captures the tension.

For the TTTEEE+lowl dataset, the remaining parameters are partially or fully limited by weak priors that allow a large volume of parameter space. In this case their posterior probabilities are highly non-Gaussian and can provide a misleading view of tension from difference in mean or related statistics. Goodness of fit statistics can also be misleading because the TTTEEE+lowl best fit can lie in regions of parameter space that are far from, yet connected to, models favored by PP and vice versa due to the weak priors.

Since the PP dataset, and any analysis that includes it, is more constraining and its posteriors more Gaussian, we adopt the update difference in mean technique introduced in [20]. Here we examine the difference in means between the PP analysis and a joint PP+TTTEEE+lowl analysis.

We isolate the linear combination of $\Theta^{(i)}$ parameters that can exhibit significant tension using a Karhunen-Loève decomposition of their covariance matrices [20]. We find that only a single combination of $\Theta^{(i)}$ can exhibit such tension and it is dominated by $\Theta^{(1)}$, with a small $\Theta^{(2)}$ component. Moreover, the significance of the shift, 1.9σ , is in good agreement with the analysis in the main text. This shows that marginalizing the additional $\Theta^{(i)}$ parameters with weak priors that encompass large parameter volumes does not artificially lower the tension.

-
- [1] A. G. Riess, S. Casertano, W. Yuan, L. M. Macri, and D. Scolnic, *Astrophys. J.* **876**, 85 (2019), arXiv:1903.07603 [astro-ph.CO].
- [2] K. C. Wong *et al.*, (2019), arXiv:1907.04869 [astro-ph.CO].
- [3] N. Aghanim *et al.* (Planck), (2018), arXiv:1807.06209 [astro-ph.CO].
- [4] G. E. Addison, D. J. Watts, C. L. Bennett, M. Halpern, G. Hinshaw, and J. L. Weiland, *Astrophys. J.* **853**, 119 (2018), arXiv:1707.06547 [astro-ph.CO].
- [5] W. L. Freedman *et al.*, (2019), 10.3847/1538-4357/ab2f73, arXiv:1907.05922 [astro-ph.CO].
- [6] W. Yuan, A. G. Riess, L. M. Macri, S. Casertano, and D. Scolnic, (2019), arXiv:1908.00993 [astro-ph.GA].
- [7] T. M. C. Abbott *et al.* (DES), *Phys. Rev.* **D98**, 043526 (2018), arXiv:1708.01530 [astro-ph.CO].
- [8] C. Chang *et al.* (LSST Dark Energy Science), *Mon. Not. Roy. Astron. Soc.* **482**, 3696 (2019), arXiv:1808.07335

- [astro-ph.CO].
- [9] C. Hikage *et al.* (HSC), *Publ. Astron. Soc. Jap.* **71**, 43 (2019), arXiv:1809.09148 [astro-ph.CO].
- [10] H. Hildebrandt *et al.*, (2018), arXiv:1812.06076 [astro-ph.CO].
- [11] S. Joudaki *et al.*, (2019), arXiv:1906.09262 [astro-ph.CO].
- [12] G. E. Addison, Y. Huang, D. J. Watts, C. L. Bennett, M. Halpern, G. Hinshaw, and J. L. Weiland, *Astrophys. J.* **818**, 132 (2016), arXiv:1511.00055 [astro-ph.CO].
- [13] N. Aghanim *et al.* (Planck), *Astron. Astrophys.* **607**, A95 (2017), arXiv:1608.02487 [astro-ph.CO].
- [14] Y. Akrami *et al.* (Planck), (2019), arXiv:1906.02552 [astro-ph.CO].
- [15] G. Obied, C. Dvorkin, C. Heinrich, W. Hu, and V. Miranda, *Phys. Rev.* **D96**, 083526 (2017), arXiv:1706.09412 [astro-ph.CO].
- [16] F. Couchot, S. Henrot-Versill, O. Perdureau, S. Plaszczynski, B. Rouill d’Orfeuille, M. Spinelli, and M. Tristram, *Astron. Astrophys.* **597**, A126 (2017), arXiv:1510.07600 [astro-ph.CO].
- [17] J. B. Muoz, D. Grin, L. Dai, M. Kamionkowski, and E. D. Kovetz, *Phys. Rev.* **D93**, 043008 (2016), arXiv:1511.04441 [astro-ph.CO].
- [18] J. Valiviita, *JCAP* **1704**, 014 (2017), arXiv:1701.07039 [astro-ph.CO].
- [19] E. Di Valentino, A. Melchiorri, and J. Silk, *Nat. Astron.* (2019), 10.1038/s41550-019-0906-9, arXiv:1911.02087 [astro-ph.CO].
- [20] M. Raveri and W. Hu, (2018), arXiv:1806.04649 [astro-ph.CO].
- [21] E. Di Valentino, A. Melchiorri, E. V. Linder, and J. Silk, *Phys. Rev.* **D96**, 023523 (2017), arXiv:1704.00762 [astro-ph.CO].
- [22] A. Heavens, Y. Fantaye, E. Sellentin, H. Eggers, Z. Hosenie, S. Kroon, and A. Mootooyaloo, *Phys. Rev. Lett.* **119**, 101301 (2017), arXiv:1704.03467 [astro-ph.CO].
- [23] S. Grandis, D. Rapetti, A. Saro, J. J. Mohr, and J. P. Dietrich, *Mon. Not. Roy. Astron. Soc.* **463**, 1416 (2016), arXiv:1604.06463 [astro-ph.CO].
- [24] W. Lin and M. Ishak, *Phys. Rev.* **D96**, 083532 (2017), arXiv:1708.09813 [astro-ph.CO].
- [25] E. Di Valentino, A. Melchiorri, and J. Silk, *Phys. Rev.* **D92**, 121302 (2015), arXiv:1507.06646 [astro-ph.CO].
- [26] B. Hu and M. Raveri, *Phys. Rev.* **D91**, 123515 (2015), arXiv:1502.06599 [astro-ph.CO].
- [27] F. Renzi, E. Di Valentino, and A. Melchiorri, *Phys. Rev.* **D97**, 123534 (2018), arXiv:1712.08758 [astro-ph.CO].
- [28] E. Di Valentino, A. Melchiorri, and J. Silk, *Phys. Rev.* **D93**, 023513 (2016), arXiv:1509.07501 [astro-ph.CO].
- [29] P. Motloch and W. Hu, *Phys. Rev.* **D97**, 103536 (2018), arXiv:1803.11526 [astro-ph.CO].
- [30] N. Aghanim *et al.* (Planck), *Astron. Astrophys.* **594**, A11 (2016), arXiv:1507.02704 [astro-ph.CO].
- [31] N. Aghanim *et al.* (Planck), (2019), arXiv:1907.12875 [astro-ph.CO].
- [32] N. Aghanim *et al.* (Planck), (2018), arXiv:1807.06210 [astro-ph.CO].
- [33] L. Pagano, J. M. Delouis, S. Mottet, J. L. Puget, and L. Vibert, (2019), arXiv:1908.09856 [astro-ph.CO].
- [34] P. A. R. Ade *et al.* (Planck), *Astron. Astrophys.* **594**, A15 (2016), arXiv:1502.01591 [astro-ph.CO].
- [35] S. Alam *et al.* (BOSS), *Mon. Not. Roy. Astron. Soc.* **470**, 2617 (2017), arXiv:1607.03155 [astro-ph.CO].
- [36] F. Beutler, C. Blake, M. Colless, D. H. Jones, L. Staveley-Smith, *et al.*, *Mon. Not. Roy. Astron. Soc.* **416**, 3017 (2011), arXiv:1106.3366 [astro-ph.CO].
- [37] A. J. Ross, L. Samushia, C. Howlett, W. J. Percival, A. Burden, and M. Manera, *Mon. Not. Roy. Astron. Soc.* **449**, 835 (2015), arXiv:1409.3242 [astro-ph.CO].
- [38] D. M. Scolnic *et al.*, *Astrophys. J.* **859**, 101 (2018), arXiv:1710.00845 [astro-ph.CO].
- [39] J. W. Henning *et al.* (SPT), *Astrophys. J.* **852**, 97 (2018), arXiv:1707.09353 [astro-ph.CO].
- [40] P. Motloch, W. Hu, and A. Benoit-Lévy, *Phys. Rev.* **D95**, 043518 (2017), arXiv:1612.05637 [astro-ph.CO].
- [41] P. Motloch and W. Hu, *Phys. Rev.* **D96**, 103517 (2017), arXiv:1709.03599 [astro-ph.CO].
- [42] R. Adam *et al.* (Planck), *Astron. Astrophys.* **596**, A108 (2016), arXiv:1605.03507 [astro-ph.CO].
- [43] A. Lewis and S. Bridle, *Phys. Rev.* **D66**, 103511 (2002), arXiv:astro-ph/0205436 [astro-ph].
- [44] A. Gelman and D. B. Rubin, *Statist. Sci.* **7**, 457 (1992).
- [45] P. Motloch and W. Hu, *Phys. Rev.* **D99**, 023506 (2019), arXiv:1810.09347 [astro-ph.CO].
- [46] J. L. Bernal, L. Verde, and A. G. Riess, *JCAP* **1610**, 019 (2016), arXiv:1607.05617 [astro-ph.CO].
- [47] K. Aylor, M. Joy, L. Knox, M. Millea, S. Raghunathan, and W. L. K. Wu, *Astrophys. J.* **874**, 4 (2019), arXiv:1811.00537 [astro-ph.CO].
- [48] K. N. Abazajian *et al.* (CMB-S4), (2016), arXiv:1610.02743 [astro-ph.CO].
- [49] G. Efstathiou and S. Gratton, (2019), arXiv:1910.00483 [astro-ph.CO].